European Journal of Pharmaceutics and Biopharmaceutics 72 (2009) 173–182

Contents lists available at ScienceDirect

European Journal of Pharmaceutics and Biopharmaceutics

journal homepage: www.elsevier.com/locate/ejpb

Research paper

Characterisation of density distributions in roller-compacted ribbons using micro-indentation and X-ray micro-computed tomography

Andres M. Miguélez-Morán [a,b], Chuan-Yu Wu [a,*], Hanshan Dong [c], Jonathan P.K. Seville [d]

[a] School of Chemical Engineering, University of Birmingham, Birmingham, UK
[b] School of Pharmaceutical Technology and Biopharmacy, University of Heidelberg, Heidelberg, Germany
[c] School of Metallurgy and Materials, University of Birmingham, Birmingham, UK
[d] School of Engineering, University of Warwick, Coventry, UK

ARTICLE INFO

Article history:
Received 9 September 2008
Accepted in revised form 8 December 2008
Available online 24 December 2008

Keywords:
Roller compaction
Granulation
Agglomeration
Micro-indentation
X-ray tomography
Density distribution
Ribbon

ABSTRACT

Roller compaction is one stage in a dry granulation process to produce free flowing granules. Its proper understanding is essential in optimising manufacturing efficiency and product quality. Roller compaction produces a compacted strip or "ribbon", which is then milled to produce granules. For a given milling condition, the density distribution in the ribbons determines the properties of the granules (particularly their size distribution and strength). Therefore, knowing the density distributions in the ribbons is very important in improving the effectiveness of the roller compaction process and the quality of the granules produced. In this paper, the density distribution in roller-compacted ribbons of microcrystalline cellulose (Avicel PH102) has been examined using three different techniques: (1) sectioning; (2) micro-indentation and (3) X-ray micro-computed tomography. It has been shown that with proper calibration all three techniques can essentially produce the same results, but with a different degree of resolution (scale of scrutiny). In addition, the influence of process conditions, such as roll gap, roll speed and the presence or absence of lubrication, on the ribbon density distributions has also been investigated. Flow into the press is often constrained by the presence of "cheek plates", which prevent lateral powder movement. In this type of arrangement, it is found that non-uniform powder feeding occurs in the compaction region, induced by the friction between the powder and the cheek plates; as a result, the densities in the middle of the ribbon width are generally higher than those close to the edges. It has also been shown that higher average ribbon densities are obtained when the roll gap, roll speed, or the friction between the powder and the side cheek plates is reduced.

© 2008 Elsevier B.V. All rights reserved.

1. Introduction

Roller compaction is one stage in a continuous dry granulation process for producing free flowing granules. In this process, powder blends are compressed between two counter-rotating rollers to form ribbons, flakes or briquettes, which are then milled to obtain granules [1,2]. Compared to other granulation processes, roller compaction has several advantages: (1) it is the most cost-effective process because of its low demand for space, personnel, energy and time consumption; (2) it is the most feasible granulation process for formulations with drugs sensitive to heat, moisture or solvents, as no liquid and additional heat are needed; (3) it is a continuous process with high throughput and relatively low energy consumption [1,2]; (4) it can produce more homogeneous products when compared to other dry granulation techniques, such as *slugging* [3,4]; and (5) it is possible to implement on-line control and automation of processing settings, so that batch-to-batch variations are minimised and the product quality is improved. Hence, roller compaction has attracted increasing attention over the last decade [1,3–14].

The properties of the granules (i.e., size distribution and strength) produced from roller-compacted ribbons depend upon the properties of the ribbons, such as density distribution and strength, and the milling conditions. Nyström and Alderborn [15] showed that the porosity and size of the granules were determined by these properties of ribbons for a given milling condition. Sheskey and Hendrey [16] showed that the change in the ribbon strength altered the grinding time in the mill to obtain granules of similar properties. In other words, under the same milling conditions, finer granules were produced with weaker ribbons (i.e., with lower tensile strength) while a larger proportion of coarse granules were obtained with stronger ribbons, as also demonstrated by many others [7,17,18]. Recent studies [19–21] revealed that the strength of compressed pharmaceutical compacts primarily depends on their relative densities, i.e., solid fraction. The

* Corresponding author. School of Chemical Engineering, University of Birmingham, Edgbaston, Birmingham B15 2TT, UK. Tel.: +44 121 4145365; fax: +44 121 4145324.
E-mail address: C.Y.WU@bham.ac.uk (C.-Y. Wu).

0939-6411/$ - see front matter © 2008 Elsevier B.V. All rights reserved.
doi:10.1016/j.ejpb.2008.12.005

variation of local densities in the ribbons will hence result in the difference in the localised ribbon strength and consequently will lead to a wide size distribution of the produced granules for a given milling condition. Therefore, knowing the density distributions of ribbons is very important in order to optimise roller compaction process, and thus to improve the quality of the granules produced. A drilling technique was developed by Funakoshi et al. [22] to estimate the compressive pressure applied to compact the powders along the roll width during roller compaction. For a given roller compaction setup, the variation in the compressive pressure would indicate the variations in ribbon density distribution. By correlating the force needed for drilling the produced compacts with the compression pressure, they found that the compression pressure in the middle of ribbon width is much higher than that at the edges, indicating that the density distribution in the compacted ribbon is not homogeneous. Nevertheless, little attention has been paid to the characterisation of density distributions of roller-compacted ribbons, although a variety of techniques, such as micro-hardness [23], mercury porosimetry [23], X-ray tomography [24,25] and NMR [26,27], have been used to characterise the density distribution of pharmaceutical tablets.

Therefore, the objectives of this paper were to characterise the variation of local density in the roller-compacted ribbons and to explore how the process conditions affect the density distributions in the ribbons. For these purposes, micro-indentation, X-ray micro-computed tomography (μCT) and sectioning methods are used to measure the local densities in the ribbons, so as to explore the local density variation. This paper is structured as follows. Firstly, the principles of micro-indentation and X-ray μCT micro will be briefly described. Secondly, the application of these techniques to characterise density distributions will be presented. Finally, the density distributions of ribbons produced under different roller compaction conditions are presented, the influence of the process conditions is discussed and the utility of the characterisation techniques employed is evaluated.

2. Micro-indentation

Micro-indentation is a technique for determining the hardness of materials at the micro-scale, which quantifies the resistance of a material to plastic deformation. During the micro-indentation test, an indenter of known shape and size is pressed into the material to be tested with a specified force. The size of the indentation depends on the dimensions of the indenter, the applied load and the hardness of the sample. The Vickers micro-hardness test used in this work is a standard micro-indentation test that uses a diamond indenter in the shape of a square-base pyramid. During Vickers tests, both diagonals of the indent are measured and the mean of these values is used to calculate the surface area of the indent, hence the hardness can be determined.

For pharmaceutical compacts, it is recognised that the local hardness is related to the local density. Generally, the higher the density is, the higher the hardness. Thus, micro-indentation tests have recently been performed to characterise the mechanical properties of pharmaceutical compacts [23,28–31]. For instance, the hardness of different compacted batches of lactose was determined by Busignies et al. [28], who showed that the hardness was indirectly proportional to the tablet porosity. The relationship between tablet density and hardness was established by Sinka et al. [29], which was used to obtain density distribution maps in the tablets produced with lubricated and non-lubricated dies. Micro-indentation was also used to examine the heterogeneity of the compact [30], to explore the effect of compaction parameters on the ribbon hardness [23] and to determine the endurance of polymeric film coating of ibuprofen tablets [31].

3. X-ray micro-computed tomography (X-ray micro-CT)

X-ray micro-CT is a non-destructive technique that provides three-dimensional images of micro-structures with a resolution of several microns. During the test, a sample is attached onto the turntable (see Fig. 1). An X-ray beam is then directed to the sample. In passing through the sample, some X-ray photons are attenuated (absorbed), whereas others will transmit through the sample and be detected by the detector. The absorption ability of a material for the X-ray photon energy is characterised using the linear attenuation coefficient μ, which can be approximated as in [32]

$$\mu = \rho \cdot \frac{Z}{A} \cdot N_{AV} \cdot \left(a + b \cdot \frac{Z^{3.8}}{E^{3.2}} \right) \quad (1)$$

where ρ is the material density, Z is the effective atomic number, A is the atomic weight, N_{AV} is Avogadro's number, a is the Klein–Nishina coefficient that is only weakly dependent on the X-ray photon energy, b is a constant with a value of 9.8×10^{24} and E is the photon energy. Thus, the linear attenuation coefficient μ depends upon the material density ρ, the atomic number Z and X-ray energy E. For a given X-ray energy and a compact of a single-component material (i.e., Z is constant), the linear attenuation coefficient is proportional to the bulk density, represented by ρ.

X-ray micro-CT has been widely used to examine the properties of powder compacts, including the density distribution [24,25,33,34], granule internal porosity distribution [35] and crack and fracture patterns inside the tablets [36,37]. Potential applications of X-ray micro-CT in pharmaceutical sciences are exemplified by Hancock and Mullarney [38]. Although this technique has been used to characterise the density distributions of the tablets [24,25], quantitative analysis of the density distribution of roller-compacted ribbons using this technique has not been reported. In this study, X-ray micro-CT is used to quantitatively determine the density distribution in the roller-compacted ribbons, to examine the effect of the process conditions on the pattern of density distributions and to explore the performance and utility of this technique in comparison with other density mapping techniques, such as the sectioning method and micro-indentation.

4. Materials and methods

Microcrystalline cellulose (MCC) of Avicel grade PH102 (FMC Biopolymer, USA) was used for all experiments. The true density of MCC was measured using helium pycnometry (AccuPyc 1330, Micrometrics®, Bedfordshire, UK). Magnesium stearate (MgSt) (Liga MF-2-V, Saville Whittle, UK) was employed as the lubricant.

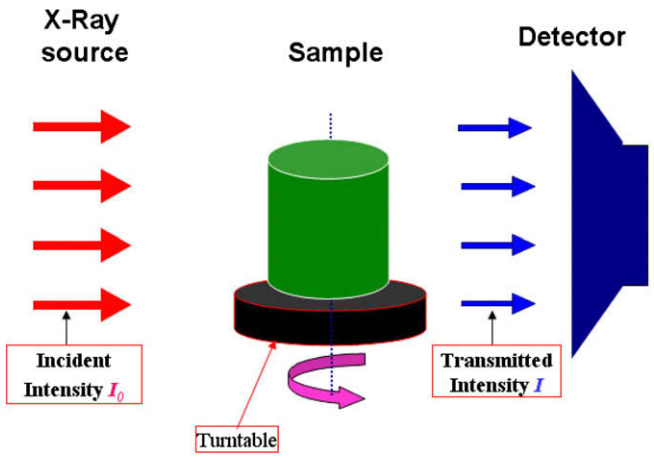

Fig. 1. Illustration of the principle of X-ray micro-computed tomography.

The compaction was carried out using a laboratory-scale instrumented roller compactor (see Fig. 2) developed at the University of Birmingham. The roll is 45 mm wide and 200 mm in diameter. The powders were fed into the compaction zone under gravity through a feeding hopper. For all roller compaction experiments reported here, the volume of powders used for each run was kept identical by feeding the powder into the hopper manually until a heap is formed above the top surface of the hopper, which was then levelled off. The ribbons were then produced under different roller compaction conditions (i.e., roll gap, roll speed and lubrication) and were then sampled for further tests in such a way that the sections at the beginning and the end of each run were discarded and only those in between were chosen, so as to minimise the effect of the powder fill level in the hopper. The density distributions in the ribbons were determined using three different methods: sectioning; micro-indentation and X-ray micro-CT.

4.1. The determination of the density using a sectioning method

The ribbons were sectioned into blocks of approximately 10×10 mm (see Fig. 3), for which the dimensions and thickness were measured using a slide calliper (CD-6 Mitutoyo, Kanagawa, Japan) and a micrometre (Digimatic Series 293, Mitutoyo, Kanagawa, Japan), respectively. The mass of each block was determined with a high precision balance (Sartorius 1702, Goettingen, Germany). Hence, the bulk densities were calculated as the ratio of the mass to the volume of the blocks. The relative densities were then calculated as the ratio of the bulk densities to the true density. For each ribbon, the bulk densities of 20 blocks were determined. The coordinates of the centre of each block were also determined for a chosen reference system. In this way, a density map that shows the variation of relative density from position to position in the ribbon was produced. Density profiles both laterally (across the ribbon width) and length wise (in the direction of motion) can also be determined by averaging the densities in each column, or row (see Fig. 3).

4.2. The determination of the density distribution using micro-indentation

Indentation experiments were performed using a micro-Vickers hardness testing system (MVK-H1, Mitutoyo, Kanagawa, Japan).

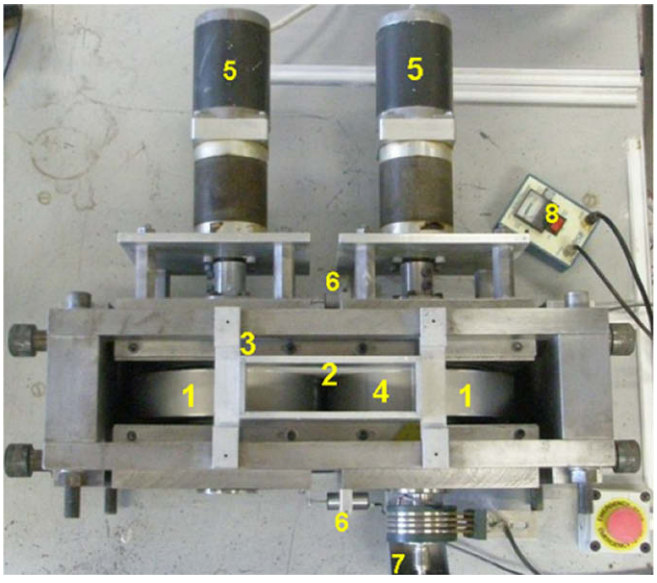

Fig. 2. The instrumented roller compactor used in this study. (1) Rollers, (2) cheek side plates, (3) hopper, (4) pressure transducer, (5) stepper motors, (6) displacement transducers, (7) encoder, (8) signal amplifier.

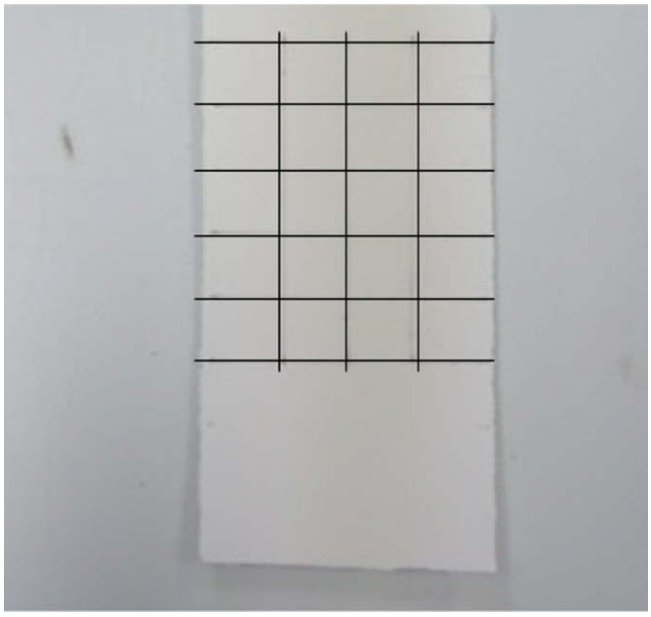

Fig. 3. Illustration of the method to section the ribbon.

The indentation load was set at 2.94 N (i.e., 300 gf) for all indentations. A typical micro-indentation pattern is shown in Fig. 4. Since the MCC ribbons do not reflect light, the indentation size and hence the hardness cannot be determined with the instrument automatically. In order to measure the indentation area, the indented specimens were first coated with a thin gold layer of 75 nm using a SC7640 sputter coater (Quorum Technologies, East Sussex, UK), then examined using an Axioskop 2 MAT reflection microscope (Zeiss, Hertfordshire, UK) equipped with a Sony XC-77 CE digital camera. The images were captured using the software AxioVision (Zeiss, Hertfordshire, UK). A fixed magnification ($5\times$) was adopted for all the specimens. The images were then digitalised and analysed using ImageJ (http://www.nih.gov). The projected surface area of each indent was determined in square pixels.

Calibration experiments were also performed to correlate the relative density with the measured micro-hardness. Eighteen calibration MCC tablets were produced using a Lloyds universal materials testing machine (Lloyd Instruments, Hampshire, UK) at six different maximum compression pressures. The thickness of the

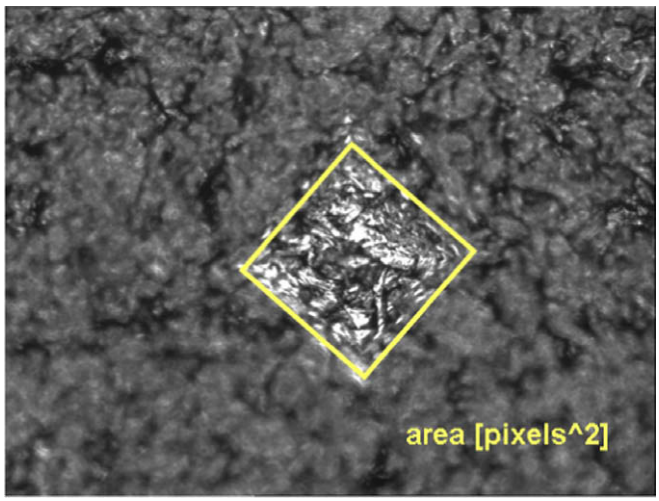

Fig. 4. A typical image of an indent on the ribbon surface with micro-indentation.

calibration tablets was controlled at around 1mm, i.e., similar to the ribbon thickness considered. The relative densities of the tablets were calculated from the mass, the volume and the true density. For each tablet, around 15 indentations were performed on the surface as shown in Fig. 5. The average indentation area was determined for each calibration tablet using the approach described above. The variation of the relative density with the average indentation area is shown in Fig. 6. It is clear that the relative density is inversely proportional to the logarithm of the average indentation area, which is consistent with the analysis of Woell [39]. A better fit to the data gives the following empirical expression:

$$d = -0.15597 \ln \psi + 2.167 \quad (2)$$

with $R^2 = 0.994$. In Eq. (2), d is the relative density, and ψ is the average indentation area (in pixel^2). Since the density of an uniaxially compressed tablet at a certain maximum compression pressure is similar to that of a ribbon produced at the same maximum compression pressure if the tablet and the ribbon have the same thickness [40,41], Eq. (2) is applicable for the MCC ribbons of approx. 1 mm thickness as considered in this paper. Therefore, the relative density at any point on the ribbon can be calculated from indentation area ψ using this equation.

Indentations were performed on the ribbon surface in a regular grid of 3 × 3 mm. The relative densities at these positions were calculated using Eq. (2) and a contour plot of the density variation in each ribbon was obtained, and the width-wise and length-wise density variations were also determined.

4.3. Determination of the density distribution using X-ray micro-CT

The produced ribbons were also examined using an X-ray micro-CT system (Skyscan 1072, Skyscan, Belgium). The X-ray beam was set at 50 kV and 98 μA. The total sample rotation was set at 180° with an interval of 0.9° (i.e., the sample was scanned every 0.9°). The spatial resolution is 11 μm/pixel for the samples considered. The reconstruction was carried out with the NRecon software (Skyscan, Kontich, Belgium). All the reconstructed images

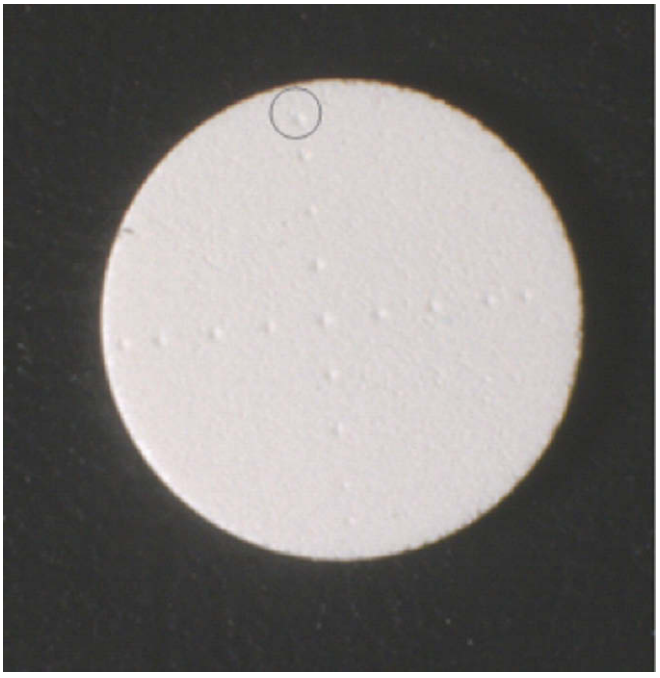

Fig. 5. A calibration tablet indented using micro-indentation.

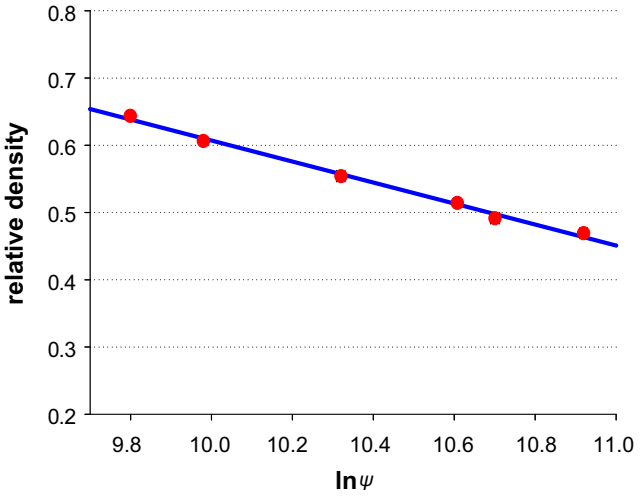

Fig. 6. Correlation between the relative density and the logarithm of the indentation area.

are shown here in pseudo colour in order to achieve a better contrast, in which the different colours represent the different attenuation coefficients. The pixel values ξ in each reconstructed X-ray micro-CT image were determined using the ImageJ software. For the determination of the average pixel value $\bar{\xi}$ of each sample, the 2D cross-section images were stacked and an integrated micro-CT image was created with the average pixel values of stacked 2D cross-section images using ImageJ. The integrated micro-CT image hence shows the average pixel values (equivalent to the linear attenuation coefficients) over the entire thickness of the sample.

In order to determine the correlation between the pixel value and the relative density, calibration experiments were also performed. The calibration tablets made at different compression pressures with the same MCC powder as used in roller compaction were examined using X-ray micro-CT, and integrated micro-CT images were produced for all the calibration tablets and are shown in Fig. 7. All the acquisition and reconstruction parameters were kept identical for all the samples. As expected, it is clear that as the maximum compression pressure increases the overall pixel value increases, indicating that the average attenuation coefficient becomes higher as the powder is compressed to a higher pressure. The relationship between the average pixel value $\bar{\xi}$ and the relative density d is shown in Fig. 8. Here, the average pixel value is linearly proportional to the relative density, which is consistent with the analysis of Sinka et al. [24] and Busignies et al. [25]. Using curve fitting, the data can be approximated as

$$d = 0.00352\bar{\xi} + 0.1584 \quad (3)$$

with $R^2 = 0.999$. It is interesting to note that Eq. (3) gives $d = 0.1584$ at the edge of the ribbon ($\bar{\xi} = 0$), which is identical to the relative density of $d = 0.16$ for non-compacted (i.e., loose packed) MCC PH102 as determined by Kumar and Kothary [42]. Using Eq. (3), the relative density at each pixel can be determined from its pixel value, and a density map can hence be constructed. Eq. (3) is used to convert the pixel values in the reconstructed micro-CT image of the ribbons into relative density distribution.

For each batch of ribbons, a sample 5 mm wide was cut across the width of one ribbon and was further sectioned into blocks of approximately 5 × 5 mm. These blocks were stacked and attached to the rotation stage of the X-ray micro-CT system, and were then scanned. For each block, reconstructed micro-CT images were obtained, and an integrated image was also created. Typical integrated images for a ribbon are shown in Fig. 9, which

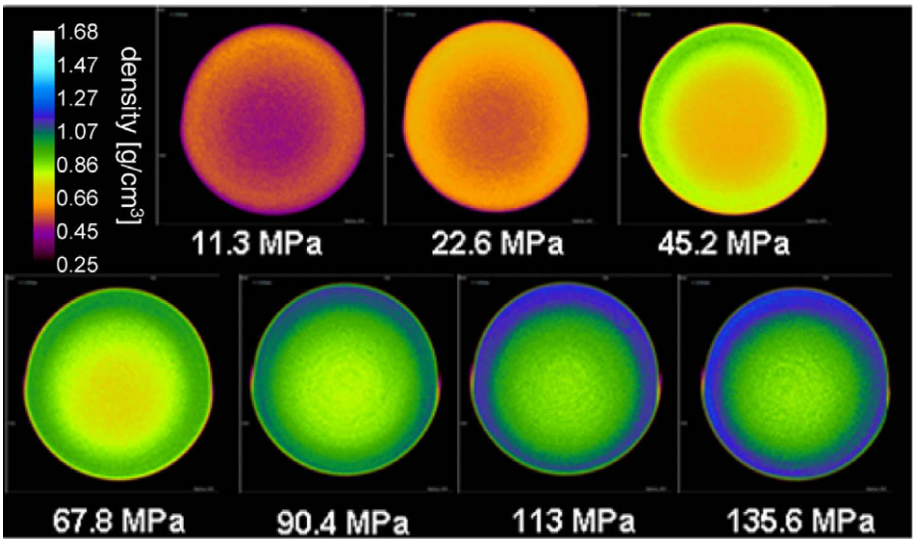

Fig. 7. The integrated X-ray micro-CT images of the calibration tablets.

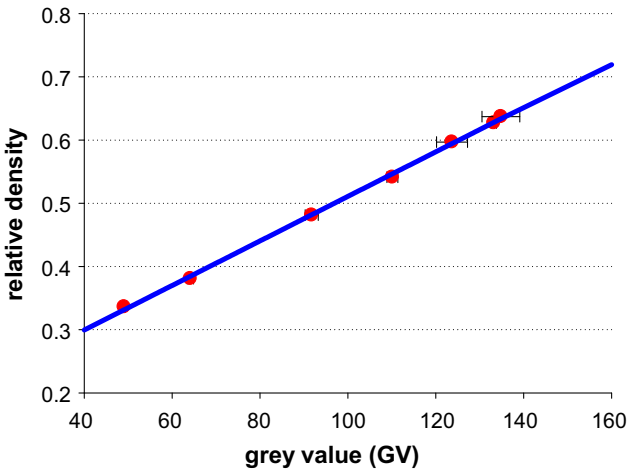

Fig. 8. Correlation between relative density and the grey values.

were further processed to generate the density mapping for the whole sample as follows. Grey values in these integrated images were averaged every 100 pixels over the sample width and were taken as data points for creating the density map. Using the calibration curve (Eq. (3)), the corresponding relative density for each data point was determined, and the density map could then be plotted together with the *x*- and *y*-coordinates of each data point. The variation of relative density across the ribbon width was also obtained by averaging the relative density in each yellow band at the same *x*-position (see Fig. 9) for all ribbons considered.

5. Results and discussion

In this study, the powder was roller compacted under different conditions in order to examine the effect of roll gap, roll speed and lubrication on the density distribution of ribbons. Four different cases were considered and are given in Table 1.

It should be noted that, for case D, the lubrication was applied in such a manner that 5% (w/w) of MgSt in ethanol was dubbed onto the surfaces of the cheek plates before the ribbons were produced. The density distributions in these ribbons and the variation of density across the ribbon width were determined using the three different methods and are shown in Figs. 10–13, respectively.

5.1. Relative density distribution in the ribbon

Figs. 10–12 show the 2D contour plots of relative density distributions in the ribbons produced. In these figures, the same colour scale is used to render the images for comparison. In the colour scale, the minimum value is set at 0.16 and the maximum is set at 0.85, which covers the entire range of relative densities for the ribbons made of MCC Avicel PH102. In other words, the chosen minimum and maximum values were the lowest and highest local relative densities among those determined for the ribbons considered. In these figures, the horizontal axis (*x*-axis) shows the position relative to the centre of the ribbon width ($r = 0$), i.e., the position is normalised by the actual ribbon width that is found to

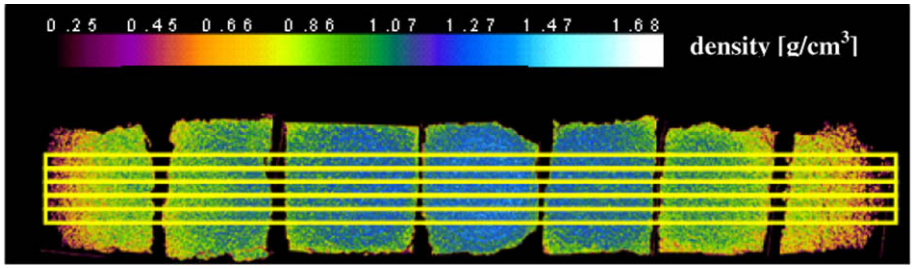

Fig. 9. Photo-montage of integrated X-ray micro-CT images for the blocks of a ribbon sample. The yellow bands show the area considered for the density mapping. (For interpretation of the references to colour in this figure legend, the reader is referred to the web version of this article.)

Table 1
The roller compaction cases investigated.

Case	Roll gap (mm)	Roll speed (rpm)	Lubrication	Ribbon width (mm)
A	1.0	6.0	No	35.4 ± 0.5
B	0.9	6.0	No	40.5 ± 0.5
C	1.0	3.0	No	40.5 ± 2.5
D	1.0	3.0	Yes	42 ± 0.5

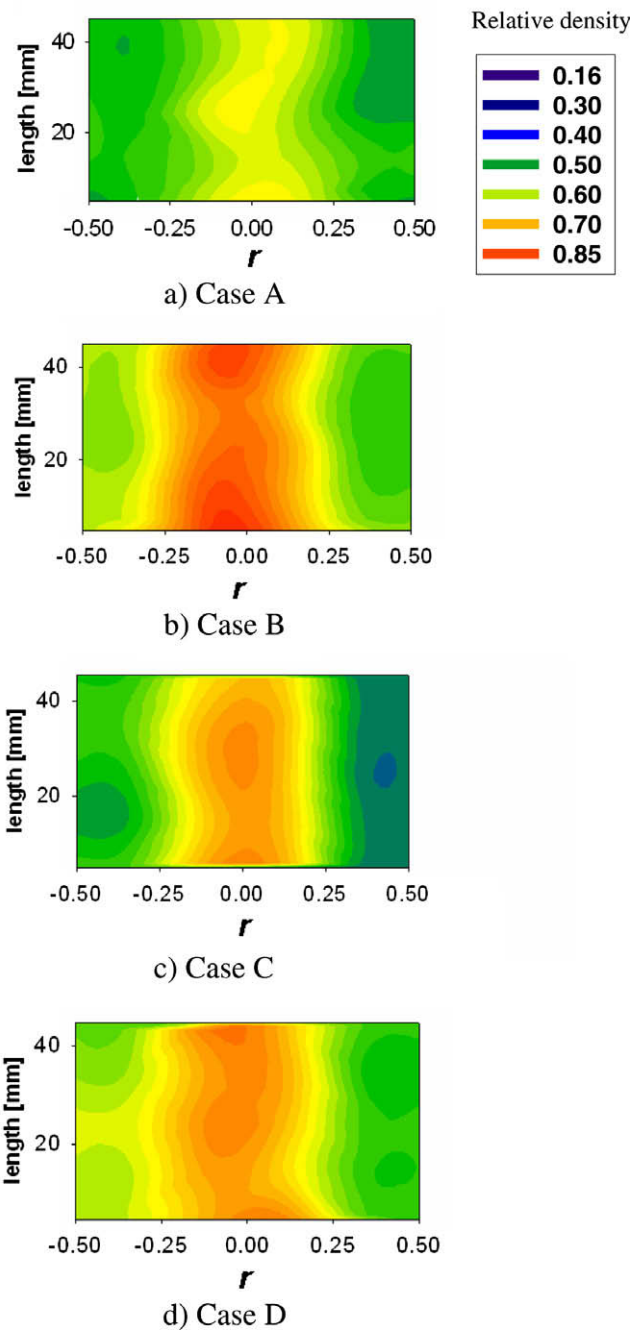

Fig. 10. Ribbon density distributions determined using the sectioning method.

vary from case to case and the actual values are given in the last column of Table 1. It is clear that under some situations, in particular, when the powder is roller compacted with a large roll gap at high roll speed, the width of the produced ribbon is less than the roll width. This is attributed to the friction between the powder and the fixed side cheek plates, which inhibits the powder situated

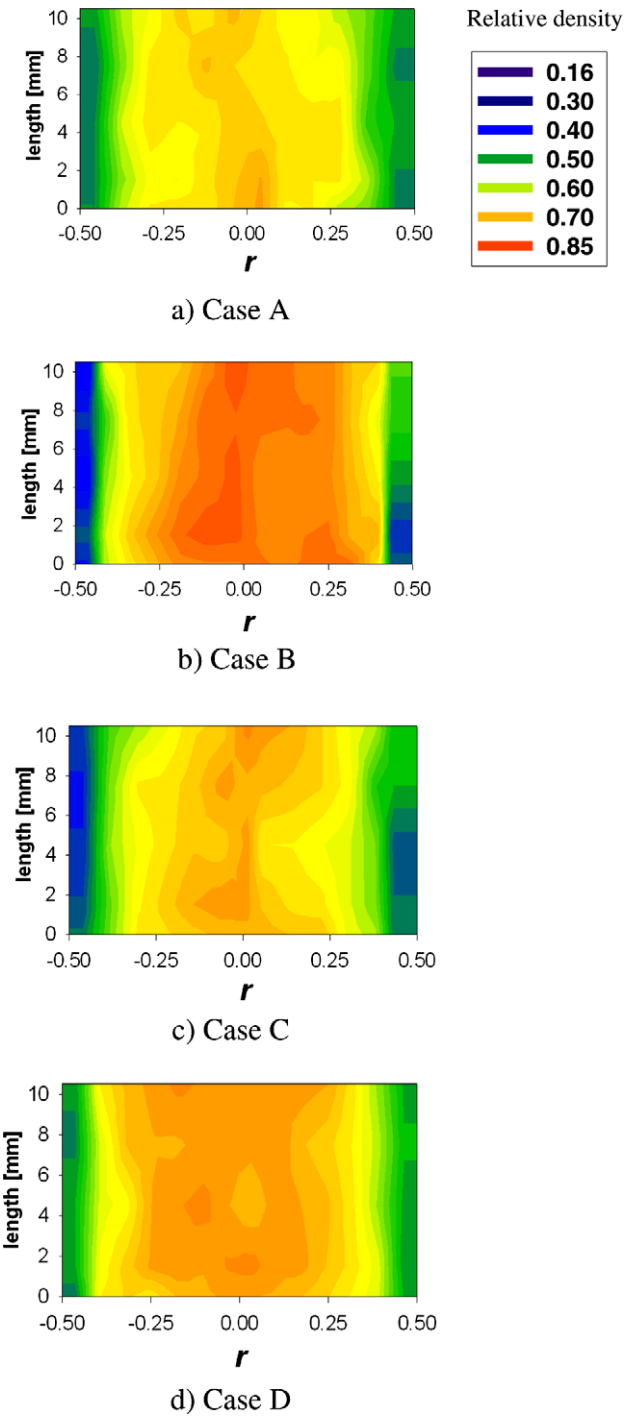

Fig. 11. Ribbon density distributions determined with micro-indentation for ribbons made at different conditions.

near the plates being gripped into the compaction zone. At large roll gap and high roll speeds, the powders in these regions are not compacted dense enough and just passes through the roll gap as flakes or even uncompacted powder. The similar phenomena were also observed by other researchers [22,40,43].

The relative density distributions determined using the sectioning method are represented in Fig. 10, in which the relative density value of each sectioned ribbon segment is plotted over the *x*- and *y*-coordinates of its central point. It can be seen that the overall patterns for all the cases considered are similar, in which higher density is induced in the middle of the ribbon width and lower

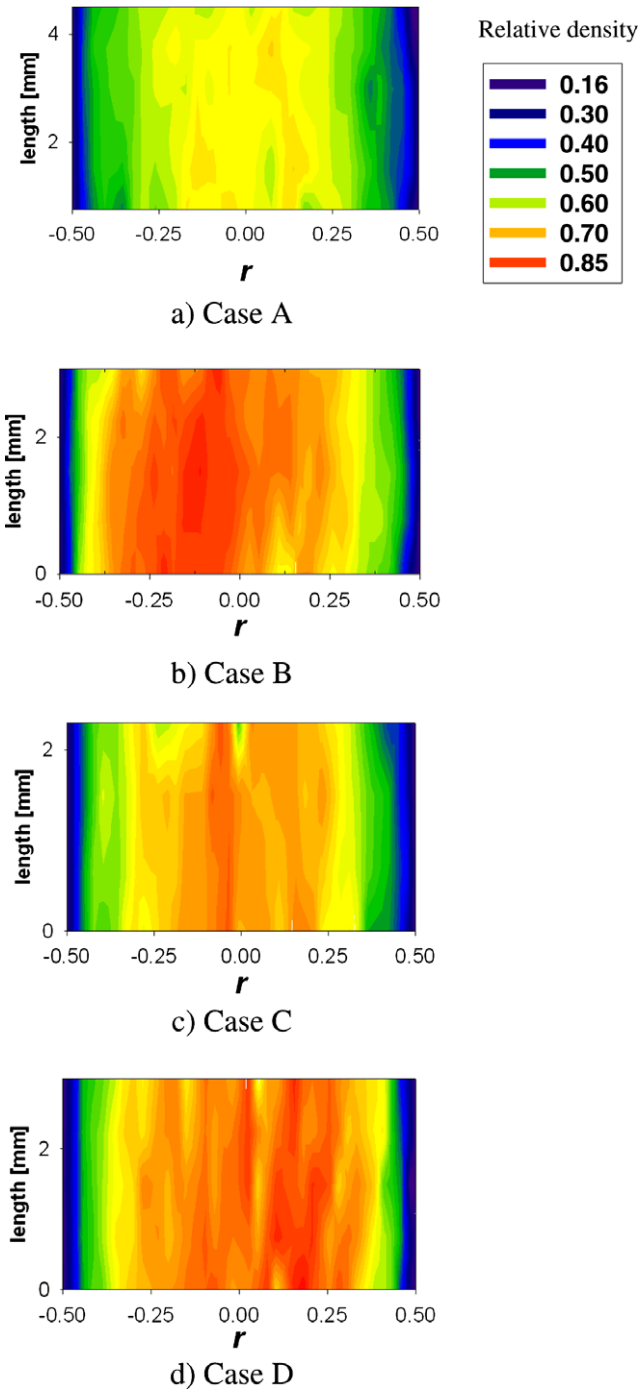

Fig. 12. Ribbon density distributions determined using X-ray micro-CT for the ribbons made at various process conditions.

density at the edges. This indicates that the powder in the middle of the ribbon width has been compressed more than that close to the edges. No significant difference in the length-wise density distribution is observed, implying that for the roller compaction performed in this study with gravity feeding, the process operates at steady state (provided that the first and last parts of the ribbon are excluded), and the length-wise density variation can be ignored. It is also clear that among the four cases considered, the overall relative densities for case B with a roll gap of 0.9 mm at a roll speed of 6 rpm (Fig. 10a) are the highest while those for case A produced at the same roll speed but with a larger roll gap of 1 mm are the lowest.

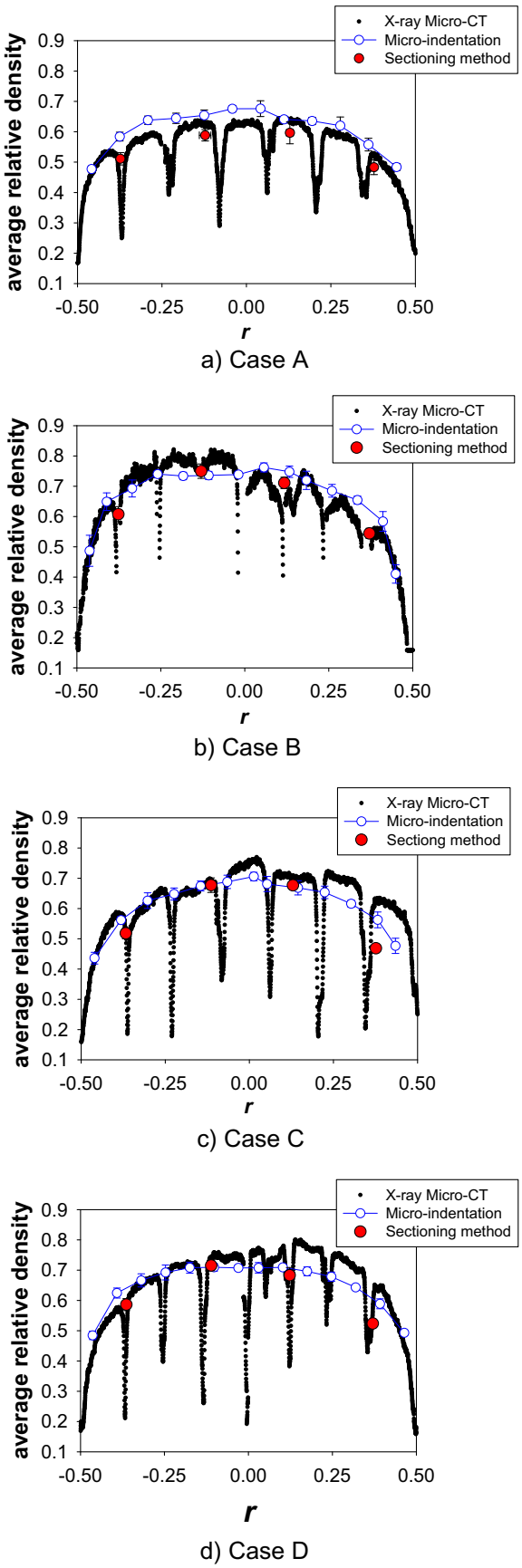

Fig. 13. Comparison of the density profiles along the ribbon width obtained using different methods.

The corresponding relative density distributions obtained using micro-indentation are shown in Fig. 11. It is clear that the overall patterns are similar to those obtained using the sectioning method, in which high densities are obtained at the middle of the ribbon while low densities at the edges. By closely examining the relative density distributions shown in Figs. 10 and 11, one can find that the local density distribution variations in a particular ribbon can be obtained with great detail using the micro-indentation method, which is due to the fact that the spatial resolution in micro-indentation (i.e., the distance between two indentations) was much smaller than the size of the segments produced using the sectioning method. The corresponding density distributions obtained using X-ray micro-CT are shown in Fig. 12. Again, similar patterns are obtained for the overall density distributions. However, due to the greater spatial resolution (around 10 μm for the samples considered here) of the X-ray micro-CT system, much more detailed information on the localised density distributions are obtained compared to the sectioning and micro-indentation methods.

5.2. The variation of average relative density across the ribbon width

It has been observed from Figs. 10–12 that the relative density in the middle of the ribbon width is much higher than that close to the edges. This is further examined by plotting the average relative densities over the ribbon length against the position along the ribbon width, as shown in Fig. 13. In this figure, the data obtained using different methods are superimposed. It is clear that different methods for determining the relative densities produce essentially identical results for all four cases considered. The dips (sharp decreases) in the density variation curves obtained using X-ray micro-CT are believed to be due to fluctuations of the pixel values at the edges of the segments, which is referred to as the edge effect. It is clear that for all cases considered, the average density in the middle of the ribbon width is higher than that at the edges. The patterns are consistent with the compressive pressure distributions obtained by Funakoshi et al. [22] and Katashinskii et al. [44]. This is a direct consequence of powder feeding patterns in the compaction region of the roller press [40]. A typical powder feed pattern is shown in Fig. 14. It can be seen that, during the roller compaction, the powders at the middle of the roller width are dragged into the compaction region at a faster rate. Consequently, a concave powder-roller interface is created, which can be quantified by a drag angle [40]. As the drag angle decreases, the powder in the middle of the roller width is dragged into the compaction zone at a faster rate. Consequently, more powder is compressed in the middle than at the rims of the roll. It is hence concluded that the heterogeneous density distribution shown in Figs. 10–13 is attributed to the powder feeding behaviour in the compaction zone, which plays a dominant role in determining the properties of roller-compacted ribbons.

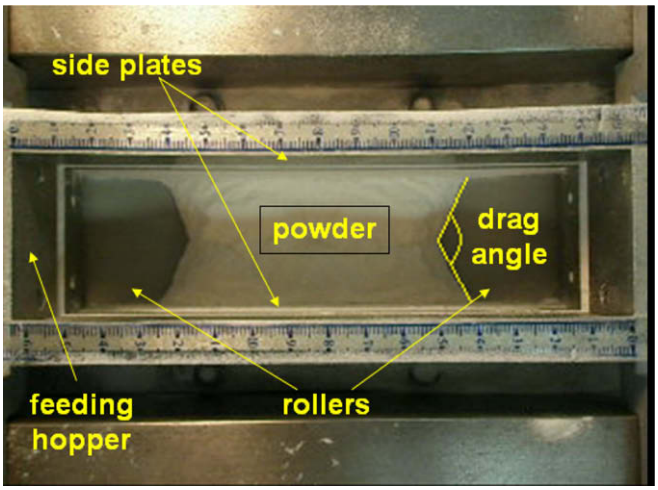

Fig. 14. Typical flow patterns of powders in the compaction zone during roller compaction.

5.3. The evaluation of various methods for determining the density distribution

Figs. 10–13 demonstrate that all three density mapping techniques are capable of determining the variation of the local relative density (solid fraction) in the ribbon with similar accuracy. However, the better the spatial resolution is, the more detailed information on the density variation can be obtained. The sectioning method is the simplest, quickest and most straightforward technique, which also allows large samples to be examined in a short time and provides a sketchy picture of the density distributions in the ribbons produced from single-component or multi-component powders. However, it is a relatively crude method and is limited to a spatial resolution (segment size) of several millimetres. It is hence difficult to obtain detailed information on the local density variation. Furthermore, the produced ribbons have to be strong enough so that they can be handled.

The spatial resolution can be improved with the micro-indentation method, using indentations at a spatial interval of 1.0 mm or less. The indentation itself can be performed fairly quickly but the determination of the indentation area using imaging analysis is a tedious and time-consuming process for most pharmaceutical materials that are non-reflective. In addition, a calibration test to correlate the relative density with the hardness or indentation size must be performed for each material to be considered. Furthermore, large samples also have to be sectioned so that the sample can be tested using some micro-indentation devices and reflection microscopes (for the systems used in this study, only samples of ca. 6 cm^2 can be tested). Although this method can be used for ribbons produced from multi-component mixtures, such as real formulations, it is incapable of characterising fragile samples, such as ribbons of very low density, for which cracks or fracture may take place even at very low indentation loads. The above limitations associated with the micro-indentation method might be addressed by using other micro-indentation or even nano-indentation systems, with which there is no need to measure the size of the indentations, the depth of indenter penetration being automatically recorded and is used to determine the hardness. Consequently, it is possible to perform automatic mapping of the hardness and hence the density distribution.

The spatial resolution can be further improved using X-ray micro-CT methods. A spatial resolution of several micrometres can be readily achieved, so that great detail of the local density variations can be obtained. However, X-ray micro-CT is only applicable for small samples so that large samples also need to be sectioned before they can be examined. Hence, the ribbon has to be strong enough to be analysed using this method. In addition, similar to micro-indentation, calibration tests have to be performed in order to correlate the pixel value of the X-ray micro-CT images to the relative density of the sample. Since X-ray micro-CT determines the linear attenuation coefficient of the material and the linear attenuation coefficient depends upon both the material density and the atomic number, which essentially represents the chemical composition of the material, caution has to be taken when this technique is used for examining ribbons composed of multi-component materials. In addition, certain artefacts in X-ray micro-CT images, such as those due to beam hardening [24,34] and the ring artefact [25], may affect the accuracy of the result generated.

In general, the use of X-ray micro-CT and micro-indentation to determine the relative density distribution demands more effort when compared to the sectioning method. The sectioning method can be used to determine the density distribution in a quick and straightforward manner. However, it requires close attention when handling the samples and the spatial resolution that can be achieved is limited. All three methods require the samples being strong enough to be handled. If coherent ribbons can be produced with multi-component formulations, both section and micro-indentation can be used to characterise the density distributions, cautions have to be taken when considering X-ray micro-CT for such a purpose as stated above.

5.4. The effect of process conditions

Since all the techniques employed in this study produce essentially the same results (see Fig. 13), the variations of average relative density across the ribbon width for various cases obtained using micro-indentation are compared in Fig. 15. In this figure, the error bars show the standard deviations of relative densities measured at the same distance from the middle of the ribbon width but at seven different points along the length of the same ribbon specimen (i.e., based on seven repetitions). It can be seen that the overall patterns for the various cases considered are similar and are consistent with the previous observations published in the literature for roller compaction with stationary cheek side plates [40] and have the same patterns as the compressive pressure determined using a drilling method [22]. It is recognised that this typical pattern is due to the influence of the friction between the powders and the cheek plates [22,40], which slows down the feeding of material into the compaction region at the rims of the rolls, as demonstrated in Fig. 14.

It is clear from Fig. 15 that when a narrower roller gap is used (case B), the average relative density is much higher than that produced with a wider roll gap at the same roll speed (case A). This is in excellent agreement with the results reported in the literature [12]. This is attributed to the fact that the powder is compressed at a much higher compaction pressure when the roll gap is reduced, so that more significant densification takes place when the powder is compressed within a narrower roll gap as evidenced in Figs. 10–12.

It can also be seen from Fig. 15 that a higher average relative density is obtained at a reduced roll speed (case C) when compared to that at higher roll speed (case A). Again, this is consistent with the results obtained by others [12]. This is believed to be due to the fact that a lower roll speed enables more entrapped air inside the powder to permeate during the roller compaction. Furthermore, the slower conveyance of the powder column into the compaction zone allows the powder particles to settle and rearrange themselves, so that the bulk powder has a higher bulk density before it is gripped into the compaction zone [40]. In addition, for plastically deformable materials, such as MCC considered in this study, a lower roll speed can also facilitate the deformation of the bulk powder and consequently increase the ribbon density.

Since the friction between the powder and side plates inhibits the feeding of the powder into the compaction zone [22], reducing the friction with lubricants will increase the feeding rate of the powder when it is compressed at the same roll speed and roll gap. Consequently, at a certain angular position inside the compaction zone, the quantity of material present is larger compared to the roller compaction without lubrication. Therefore, denser ribbons can be produced. This is demonstrated by comparing case D with case C in Fig. 15 and Figs. 10–12. It is clear that a higher average relative density across the ribbon width is obtained when the side cheek plates are lubricated with MgSt (case D), when compared to case C.

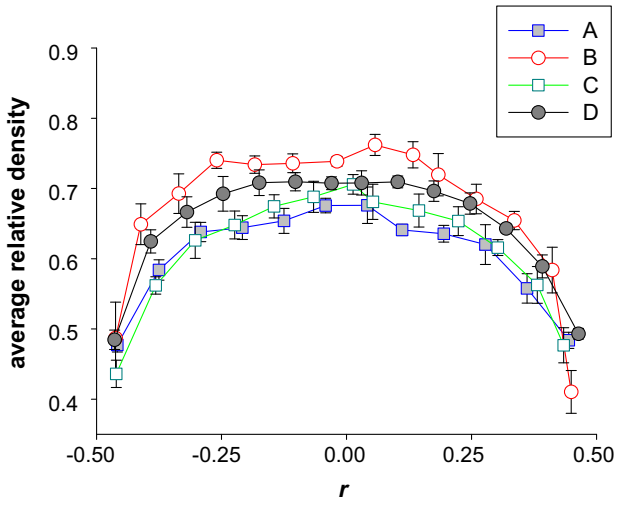

Fig. 15. The influence of process conditions on the density variation along the ribbon width obtained using micro-indentation.

6. Conclusions

In this study, three different techniques, sectioning, micro-indentation and X-ray micro-CT, have been employed to determine the density distributions in roller-compacted MCC ribbons. It has also been shown that with proper calibration to correlate the micro-hardness and the X-ray image pixel values with the relative density for micro-indentation and X-ray micro-CT, respectively, all three techniques are capable of quantifying the variations of densification across the sample but with different degrees of resolution. The sectioning method is a quick and simple technique, which can be used to obtain the density distribution of ribbons with a spatial resolution of several millimetres. When a fine resolution is needed to distinguish the local density variation, micro-indentation and X-ray micro-CT would be the preferable techniques, as both techniques can give better resolutions than the sectioning method. Sectioning and micro-indentation can also be used to examine the density distributions of the ribbons produced with multi-component mixtures but it will be inappropriate to use X-ray micro-CT because both density and chemical compositions of the mixture will contribute to the X-ray attenuation coefficient and hence the pixel values of CT images, especially when the chemical compositions of individual constituents become dominant in determining the X-ray attenuation. All three techniques can only be used for the ribbons or compacts that are strong enough to to be handled during the measurements.

It has also been shown that, due to the friction between the powder and the fixed side cheek plates, which results in non-uniform powder feeding in the compaction region, a higher density is obtained in the middle of the ribbon width when compared to those close to the edges of the ribbon. In addition, the effects of different process conditions (roll gap, roll speed and lubrication) on the density distribution have been investigated. It has been found that the ribbon density increases as the roll gap, roll speed or the friction between the powder and the side cheek plates decreases.

Acknowledgements

A.M.M. is very grateful for the support of Dr. M. Bultmann and Prof. G. Fricker. C.Y.W. would like to acknowledge the financial

support provided by the Engineering and Physical Sciences Research Council, United Kingdom, through the EPSRC Advanced Research Fellowship Scheme (Grant Nos.: EP/C545230 and EP/C545249).

References

[1] G. Shlieout, R.F. Lammens, P. Kleinebudde, Dry granulation with a roller compactor. Part I: The functional units and operation modes, Pharm. Technol. Eur. (2000) 25–35.
[2] C. Vervaet, J.P. Remon, Continuous granulation in the pharmaceutical industry, Chem. Eng. Sci. 60 (2005) 3949–3957.
[3] E.L. Parrott, Densification of powders by concavo-convex roller compactor, J. Pharm. Sci. 70 (3) (1981) 288–291.
[4] R.W. Miller, Handbook of Pharmaceutical Granulation Technology, Marcel Dekker, Inc., New York, Basel, 1997. pp. 100–148 (Chapter 6).
[5] P. Guigon, O. Simon, K. Saleh, G. Bindhumadhavan, M.J. Adams, J.P.K. Seville, Handbook of Powder Technology, vol. 11, Granulation Elsevier, Amsterdam, 2007. pp. 256–286.
[6] P. Kleinebudde, Roll compaction/dry granulation: pharmaceutical applications, Eur. J. Pharm. Biopharm. 58 (2004) 317–326.
[7] W. Weyenberg, A. Vermeire, J. Vandervoort, J.P. Remon, A. Ludwig, Effects of roller compaction settings on the preparation of bioadhesive granules on ocular minitablets, Eur. J. Pharm. Biopharm. 59 (2005) 527–536.
[8] P. Guigon, O. Simon, Interaction between feeding and compaction during lactose compaction in a laboratory roll press, KONA 18 (2000) 131–138.
[9] P. Guigon, O. Simon, Correlation between powder-packing properties and roll press compact heterogeneity, Powder Technol. 130 (1–3) (2003) 41–48.
[10] O. Simon, P. Guigon, Roll press design – influence of force feed systems on compaction, Powder Technol. 130 (1–3) (2003) 257–264.
[11] G. Bindhumadhavan, J.P.K. Seville, M.J. Adams, R.W. Greenwood, S. Fitzpatrick, Roll compaction of a pharmaceutical excipient: experimental validation of rolling theory for granular solids, Chem. Eng. Sci. 60 (2005) 3891–3897.
[12] R.F. Mansa, R.H. Bridson, R.W. Greenwood, H. Barker, J.P.K. Seville, Using intelligent software to predict the effects of formulation and processing parameters on roller compaction, Powder Technol. 181 (2) (2008) 217–225.
[13] M. Herting, P. Kleinebudde, Roll compaction/dry granulation: effect of raw material particle size on granule and tablet properties, Int. J. Pharm. 338 (1–2) (2007) 110–118.
[14] A.V. Zinchuk, M.P. Mullarney, B.C. Hancock, Simulation of roller compaction using a laboratory scale compaction simulator, Int. J. Pharm. 269 (2004) 403–415.
[15] C. Nystrom, G. Alderborn, Bonding surface area and bonding mechanism: two important factors for understanding of powder compactability. The compaction behaviour of pharmaceutical materials, Drug Dev. Ind. Pharm. 19 (17–18) (1993) 2143–2196.
[16] P.J. Sheskey, J. Hendren, The effects of roll compaction equipment variables granulation technique and HPMC polymer level on a controlled-release matrix model drug formulation, Pharm. Technol. 23 (1999) 90–106.
[17] S. Inghelbrecht, J.P. Remon, Reducing dust and improving granule and tablet quality in the roller compaction process, Int. J. Pharm. 171 (1998) 195–206.
[18] S.G. von Eggelkraut-Gottanka, S.A. Abed, W. Mueller, P.C. Schmidt, Roller compaction and tabletting of St. John's wort plant dry extract suing a gap width and force controlled roller compactor. I: Granulation and tabletting of eight different extract batches, Pharm. Dev. Technol. 7 (4) (2002) 433–445.
[19] C.K. Tye, Ch.C. Sun, G.E. Amidon, Evaluation of the effects of tabletting speed on the relationships between compaction pressure tablet tensile strength and tablet solid fraction, J. Pharm. Sci. 94 (3) (2005) 465–472.
[20] C.-Y. Wu, S.M. Best, A.C. Bentham, B.C. Hancock, W. Bonfield, A simple predictive model for the tensile strength of binary tablets, Eur. J. Pharm. Sci. 25 (2005) 331–336.
[21] C.-Y. Wu, S.M. Best, A.C. Bentham, B.C. Hancock, W. Bonfield, Predicting the tensile strength of multi-component pharmaceutical tablets, Pharm. Res. 23 (8) (2006) 1898–1905.
[22] Y. Funakoshi, T. Asogawa, E. Satake, Use of a novel roller compactor with a concavo-convex roller pair to obtain uniform compacting pressure, Drug Dev. Ind. Pharm. 6 (3) (1977) 555–573.
[23] F. Freitag, K. Reincke, J. Runge, W. Grellmann, P. Kleinebudde, How do roll compaction/dry granulation affect the tableting behaviour of inorganic materials? Microhardness of ribbons and mercury porosimetry measurements of tablets, Eur. J. Pharm. Sci. 22 (4) (2004) 325–333.
[24] I.C. Sinka, S.F. Burch, J.H. Tweed, J.C. Cunningham, Measurement of density variations in tablets using X-ray computed tomography, Int. J. Pharm. 271 (1–2) (2004) 215–224.
[25] V. Busignies, B. Leclerc, P. Porion, P. Evesque, G. Couarraze, P. Tchoreloff, Quantitative measurements of localized density variations in cylindrical tablets using X-ray microtomography, Eur. J. Pharm. Biopharm. 64 (1) (2006) 38–50.
[26] A. Djemai, I.C. Sinka, NMR imaging of density distributions in tablets, Int. J. Pharm. 319 (1–2) (2006) 55–62.
[27] V. Busignies, P. Porion, B. Leclerc, P. Evesque, P. Tchoreloff, Application of PGSTE-NMR technique to characterize the porous structure of pharmaceutical tablets, Eur. J. Pharm. Biopharm. 69 (3) (2008) 1160–1170.
[28] V. Busignies, P. Tchoreloff, B. Leclerc, C. Hersen, G. Keller, Compaction of crystallographic forms of pharmaceutical granular lactoses. II: Compacts mechanical properties, Eur. J. Pharm. Biopharm. 58 (2004) 577–586.
[29] C. Sinka, J.C. Cunningham, A. Zavaliangos, Analysis of tablet compaction. II: Finite element analysis of density distributions in convex tablets, J. Pharm. Sci. 93 (8) (2004) 2040–2053.
[30] J. Lee, Structural heterogeneity of pharmaceutical compacts probed by micro-indentation, J. Mater. Sci.: Mater. Med. 19 (2008) 1981–1990.
[31] B.D. Rohera, N.H. Parikh, Influence of plasticizer type and coat level on Surelease film properties, Pharm. Dev. Technol. 7 (4) (2002) 407–420.
[32] E.C. McCullough, Photon attenuation in computed tomography, Med. Phys. 2 (6) (1975) 307–320.
[33] D.H. Phillips, J.J. Lannutti, Measuring physical density with X-ray computed tomography, NDT&E Int. 30 (6) (1997) 339–350.
[34] S. Burch, Measurement of density variations in compacted parts using X-ray computerised tomography, MPR (2002) 24–28.
[35] L. Farbera, G. Tardosb, J.N. Michaelsa, Use of X-ray tomography to study the porosity and morphology of granules, Powder Technol. 132 (2003) 57–63.
[36] C.Y. Wu, O.M. Ruddy, A.C. Bentham, B.C. Hancock, S.M. Best, J.A. Elliott, Modelling the mechanical behaviour of pharmaceutical powders during compaction, Powder Technol. 152 (1–3) (2005) 107–117.
[37] C.-Y. Wu, B.C. Hancock, A. Mills, A.C. Bentham, S.M. Best, J.A. Elliott, Numerical and experimental investigation of capping mechanisms during pharmaceutical tablet compaction, Powder Technol. 181 (2) (2008) 121–129.
[38] B.C. Hancock, P. Mullarney, X-ray micro-tomography of solid dosage forms, Pharm. Technol. (2005) 92–100.
[39] F. Woell, Ph.D. Dissertation, Entwicklung von Methoden zur Charakterisierung von Schuelpen, University of Halle, Germany, 2003.
[40] A.M. Miguélez-Morán, C.-Y. Wu, J.P.K. Seville, The effect of lubrication on density distributions of roller compacted ribbons, Int. J. Pharm. 362 (2008) 52–59.
[41] B. Michel, Ph.D. Dissertation, Contribution a l'etude de l'agglomeration des pourdres en presse a rouleaux lises, Universite de Compiegne, France, 1994.
[42] V. Kumar, S.H. Kothary, Effect of compressional force on the crystallinity of directly compressible cellulose excipients, Int. J. Pharm. 177 (2) (1999) 173–182.
[43] U. Lubjuhn, U. Sander, K. Schoenert, Pressure profile in the compression zone of the high-pressure roller mill, ZKG 47 (1994) 157–163 (English translation).
[44] V.P. Katashinskii, G.A. Vinogradov, G.Ya. Kalutskii, Nonuniformity of stress and strain distribution over the width of rolled powder strip, Poroshkovaya Metallurgiya 12 (156) (1975) 28–32 (Translated).